JEE Journal of Ecological Engineering

Journal of Ecological Engineering, 2025, 26(6), 410–423
https://doi.org/10.12911/22998993/202322
ISSN 2299–8993, License CC-BY 4.0

Received: 2025.01.10
Accepted: 2025.04.07
Published: 2025.04.15

Development of a computational tool for stormwater management in small urban catchments

Anita Białek[1*], Anna Musz-Pomorska[2]

[1] Faculty of Environmental Engineering, Geomatics and Renewable Energy, Kielce University of Technology, Al. Tysiąclecia Państwa Polskiego 7, 25-314 Kielce, Poland
[2] Faculty of Environmental Engineering and Energy, Lublin University of Technology, Nadbystrzycka 38D, 20-618 Lublin, Poland
* Corresponding author's e-mail: anita_bialek@interia.eu

ABSTRACT

This study presents a computational tool for designing and evaluating stormwater management devices in small urban catchments. The tool is highly versatile, supporting the testing of diverse hydrological models tailored to local conditions. It is particularly useful for designing retention tanks, sizing infiltration trench, and modernizing stormwater drainage systems. Using rainfall data from 32 cities across Poland, the study highlights the influence of regional rainfall patterns on the capacity of infiltration trenches. The highest soil capacity was observed during 15-minute convective rainfall events, with a maximum of 86 m³ in Nowy Sącz and a minimum of 37 m³ in Zakopane, influenced by the unique topographical conditions of mountainous areas. These findings underscore the need for a localized approach to stormwater system design, considering terrain and rainfall intensity. The tool facilitates sustainable stormwater management strategies, improving flood prevention and urban resilience amid dynamic climate change.

Keywords: water retention, computational tool, infiltration trench, infiltration capacity.

INTRODUCTION

Amid progressing climate change and rapid urbanization, managing stormwater in cities has become an increasingly significant challenge. Intensifying rainfall, more frequent flooding, and hydrological changes driven by rising temperatures are compromising the performance of urban water infrastructure (Gill et al., 2007; Denault et al., 2006; Taguchi et al., 2020). Urbanization exacerbates these issues by increasing impervious surfaces, such as roads and buildings, which accelerate stormwater runoff and reduce retention capacity (Chen et al., 2021; Miller et al., 2014). These phenomena underscore the urgent need to modernize urban catchments to adapt to evolving climatic conditions and the pressures of urban growth (Szeląg et al., 2022a; Musz-Pomorska and Widomski, 2022). The "sponge cities" concept, pioneered in China, offers a modern and sustainable approach to urban water management. This approach envisions cities functioning like sponges, storing rainwater and releasing it gradually (Jiang et al., 2018; Song, 2022). The goal is to mitigate flood risks while enhancing water availability during drought periods (Wang et al., 2018; Ursino, 2015). A key component of this model is the integration of green-blue infrastructure with urban hydrological systems. This includes solutions such as green roofs, parks, infiltration trenches, and retention tanks, which can reduce flood risks by 30–50% compared to traditional sewer systems (Chan et al., 2018; Zhang et al., 2019; Czerpak and Widomski, 2024).

Practical examples from Chinese cities like Shenzhen and Chongqing demonstrate that these solutions improve local water retention and positively impact water resource management (Jiang et al., 2018). Nature-Based Solutions (NBS) in urban environments are gaining prominence. These solutions – retention tanks, infiltration trenches, rain gardens, and green roofs – not only enhance water retention but also improve urban environmental quality. For example, infiltration trenches and other natural infiltration systems enable water to seep into the soil, reducing rapid surface runoff and stabilizing the local water balance (Kabisch et al., 2017). Similarly, rain gardens act as natural filters, capturing pollutants before they enter sewer systems, thereby significantly improving urban water quality (Hatt et al., 2004).

In addition to mitigating flood risks, green-blue infrastructure improves urban microclimates, counteracting the urban heat island effect (Shariat et al., 2019). Notable examples of successful adaptation include Rotterdam, where a stormwater management system retains up to 10 million m³ of water annually, reducing runoff by 25% by Boogaard et al. (2024). In Melbourne, the "Urban Forest Strategy" expanded green space by 40%, reducing daytime urban temperatures by 1 °C to 3.8 °C through an increase in green roof coverage from 30% to 90%, effectively mitigating the urban heat island effect (Imran et al., 2018; City of Melbourne, 2012).

Modern tools for modelling catchments and retention systems, such as the Storm Water Management Model (SWMM), Model for Urban Stormwater Improvement Conceptualization (MUSIC), Modular Online Simulation Engine (MOUSE), and MIKE URBAN (a software suite developed by DHI for integrated urban water modelling, with "MIKE" referring to the Danish Hydraulics Institute), enable more effective planning and design of NBS by Hansen et al. (2014). SWMM, a widely utilized tool, provides detailed hydrological and hydraulic analyses of sewer systems, aiding in the evaluation of implemented solutions (Wu et al., 2020; Farina et al., 2023). MUSIC, particularly popular in Australia, simulates critical processes such as infiltration and sedimentation, essential for NBS. MIKE URBAN offers a comprehensive approach to urban hydrology modelling by integrating various stormwater management systems, though its technical complexity and high costs limit broader adoption (US EPA, 2015). Also diverse new approaches, algorithms and numerical methods are described as possible to apply in modelling of integrated urban water management system (Łazuka et al., 2022).

Despite these advanced tools, guidelines for designing and implementing NBS often remain incomplete and are not adapted to local climatic and infrastructural conditions, especially in Central and Eastern Europe (Kabisch et al., 2017). These gaps contribute to inadequate stormwater management, as evidenced by the 2021 floods in Western and Central Europe, which caused significant material losses (European Environment Agency, 2015).

Studies from Italy and the USA highlight the importance of modern stormwater management strategies in the context of climate change. For example, Milan's "Milan Green Plan" increased the number of green roofs and rain gardens, improving water retention and mitigating the urban heat island effect. Research (Marchioni et al., 2018; Procaccini and Monticelli, 2021; Salerno et al., 2021; Sanesi et al., 2016) shows that such solutions significantly reduce surface stormwater runoff and enhance urban water quality.

In the United States, cities like New Orleans and Houston, vulnerable to intense rainfall and hurricanes, have implemented extensive retention systems. Following Hurricane Katrina in 2005, New Orleans invested in advanced infiltration trenches and retention tanks. Regulations under Low Impact Development (LID) required developers to incorporate solutions such as green roofs and permeable surfaces, greatly improving stormwater management (Davis et al., 2012; Maimone et al., 2011).

Stormwater management remains a critical challenge in Poland and globally amidst rapid climate change and urbanization. In Poland, outdated sewer infrastructure and insufficient retention capacity emphasize the urgent need for modernization (Szeląg at al. 2022b). Adopting innovative models like China's "sponge cities" could significantly improve water retention and urban resilience to extreme weather events, including floods and droughts (Song et al., 2022; Xing et al., 2019). NBS offer a modern approach by integrating hydrological functions with urban planning, thereby enhancing cities' adaptive capacity.

This article introduces a proprietary computational application for designing, assessing, and modernizing selected NBS structures, such as detention basins, infiltration basins, infiltration trenches, and rain gardens. The developed tool integrates with existing computational software, which often provides limited support for NBS solutions, offering a distinct advantage. The application was used to evaluate the impact of regional rainfall conditions across Poland on the retention capacity of infiltration trenches. The diverse hydrological conditions in different regions underscore the need for a tailored approach to stormwater system design to improve efficiency and resilience against extreme weather events. This tool contributes to the development of modern stormwater management strategies, strengthening urban ecosystems' resilience to climate change. Its application is vital for promoting sustainable development and ensuring hydrological safety in Poland and beyond.

METHODS AND DATA

Rainfall data and regional convection rainfall models

Rainfall data were collected from 32 meteorological stations located in various Polish cities (meteorological stations belonging to the IMGW-PIB network). Poland's climate (Central Europe), classified as temperate warm, exhibits a transitional nature between the marine characteristics of Western Europe and the continental characteristics of Eastern Europe. This results in the influx of air masses with varying thermal and humidity properties, leading to considerable variability in rainfall limit (Niedźwiedź et al., 2009; Szeląg et al., 2022b). The average annual rainfall in Poland (1981–2010) is approximately 600 mm, ranging from 520 mm in the central regions to nearly 700 mm along the Baltic coast and over 1000 mm in the mountains. The heaviest rainfall occurs from May to August, with July experiencing the highest frequency of rainfall.

The selection of rainfall stations ensured even spatial distribution across Poland, representing diverse physiogeographical conditions such as mountains, foothills, uplands, lowlands, lakes, and the coastal zone (Fig. 1).

When modelling rainfall in small urban catchments, it is essential to consider short-duration, high-intensity rainfall events, primarily associated with atmospheric convection (Kupczyk and Suligowski, 1997; Łupikasza, 2016). These events typically have a limited spatial extent (up to 10 km²) and high intensity. In Poland, such rainfall events generally last up to 90 minutes (coefficient values of $a_1 < 2.8 \cdot 10^{-3}$ and $a_2 > 0.31$ – more information in S1 Table). On the basis of the literature data reported by Szeląg et al. (2022b), convective rainfall events during the summer half-year (May – October) from 1961 to 2005 were identified using traditional pluviograph records. A four-hour gap between rainfall events was used as the defining interval (Kupczyk and Suligowski, 2000; DWA-A 118E, 2006).

The highest frequency of convective events was recorded in mountainous regions and along the Baltic coast, though their average intensity was relatively low (< 0.6 mm). Over 65% of these events lasted up to 30 minutes, with frequency decreasing as duration increased. To accurately reflect the temporal variability of rainfall

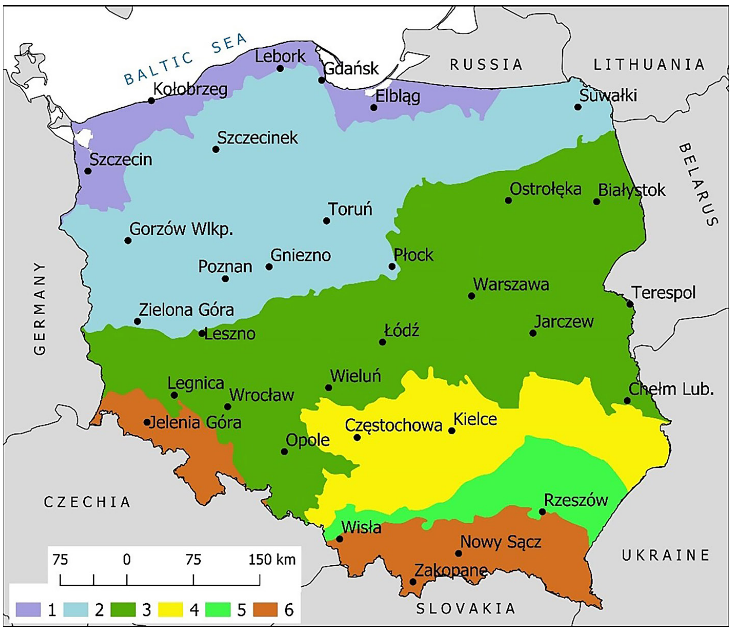

Figure 1. Location of rain gauges against the background of the main physical-geographical regions of Poland (1 – Baltic coastal lowlands, 2 – lakelands, 3 – central lowlands, 4 – uplands, 5 – sub-mountain basins, 6 – mountains)

events, 5-minute intervals were applied, ensuring that the dataset captured several episodes per year over the multi-year analysis period. For all measurement points, the 45 highest rainfall event values were selected using the peak-over-threshold method, regardless of the year of occurrence (Malihout et al., 2013).

For each rainfall station, the relationship between the rainfall depth (P) and its duration (t_r) was determined. This relationship was derived using a second-degree polynomial function to calculate the probability of stormwater flooding for the characteristics of the assumed urban catchment, based on the regional convection rainfall models determined, as described in Equation 1:

$$P_{max}(t_r) = a_1 \cdot t_r^2 + a_2 \cdot t_r + a_0 \quad (1)$$

This approach has been previously validated in hydrological studies (Kupczyk and Suligowski, 1997; Szeląg et al., 2022b).The empirical coefficients a_1, a_2, and a_0 and are provided in S1 Table. The analysis revealed that average rainfall depth for convective events increases with duration, peaking at approximately 60 minutes.

Regions with the greatest increases in average rainfall depth include central Poland (e.g., Jarczew, Leszno, Łódź, Warsaw), the lake districts (e.g., Gniezno, Poznań, Suwałki), and southeastern areas (e.g., Nowy Sącz, Rzeszów). Local topography and dynamic meteorological conditions significantly influence this distribution (Szelag et al., 2022c; Kaczmarek, 2019). Conversely, the most stable rainfall patterns with the lowest maximum intensity were observed in Kielce, Częstochowa, Wieluń, Elbląg, and Kołobrzeg. Urban heat island effects and aerosols in lowland agglomerations (e.g., Białystok, Poznań, Łódź) reduce rainfall intensity, as does the evaporation effect from the sea surface in coastal cities like Szczecin and Gdańsk.

In the applied hydrological method, unit hydrographs were employed. Rainfall data were input as pulses characterized by durations (minutes), depths (mm), and intensities (mm/min). Various scenarios for convective rainfall durations ranging from 15 to 60 minutes were applied in the analysis. Rainfall events lasting up to 60 minutes with depths exceeding 0.2 mm exhibited high variability. During the studied summer period, between 1615 and 2532 such events were recorded, averaging 36–56 events per year (Szelag et al., 2022b).

Tool to modelling of NBS (Calculator_NBS)

The developed application enables forecasting of surface runoff using the kinematic wave model (Chow et al., 1998; Singh, 1996) and its transformation through various NBS structures (Raymond et al., 2017), such as retention tanks, infiltration basins, rain gardens, and infiltration trenches (EPA, 2015). This approach facilitates the design, evaluation, and modernization of NBS solutions under urban catchment conditions and in the context of climate change. Given the limited availability of data on land use and topography, the application allows for the incorporation of custom inflow hydrograph shapes for NBS structures (European Commission, 2015). The sizing of these structures is based on identifying limiting factors such as maximum runoff and water depth in the soil, ensuring accurate capacity design. The developed tool (Calculator_NBS) was used to predict the dimensions of infiltration trenches for 32 rainfall stations in Poland for convective rainfall.

The application's sizing algorithm for green infrastructure objects is implemented in C++ programming language using the Qt Creator integrated development environment (IDE). High-resolution simulation capabilities enhance the numerical stability of the solution algorithm and minimize simulation errors.

Balance equation for green infrastructure objects (Calculator_NBS)

The balance equation has been widely applied in hydrological studies to assess the efficiency of green infrastructure in managing stormwater, as emphasized in the works of the European Commission (2015) and Beven et al. (2012). Bhaskar et al. (2016) discussed the use of the balance for green infrastructure objects in calculations, which formed the basis for analyzing water flow in stormwater sewage systems. The balance Equation 2 for green infrastructure objects can be expressed as follows:

$$\begin{gathered} dV = Q_{outS}(t)dt - Q_{out}(t)dt - \\ -Q_{inf}(t)dt - ET(t)dt \end{gathered} \quad (2)$$

where: the input data include: $Q_{outS}(t)$ – inflow of water to the green infrastructure object at time t, (m^3/s), $Q_{out}(t)$ – runoff from the substrate at time t, including the flow to the ground, with overflow occurring if the allowable hydraulic capacity is exceeded, (m^3/s), $Q_{inf}(t)$ – volume of water flowing to the ground per unit time t, (m^3/s), $ET(t)$ – evapotranspiration from the surface layer, (m^3/s).

The computational diagram of the infiltration system, as outlined by Piazza and Ursino (2022) and Błażejewski at al. (2018), is illustrated in Figure (Fig. 2), providing a clear visualization of water flow dynamics within the system. The presented diagram (Fig. 2) illustrates a system consisting of an impervious sub-catchment (runoff surface) that converts rainfall into runoff, and a permeable infiltration trench (surface $B \cdot L$) where infiltration occurs.

The initial form of Equation 2 for the soil, presented as Equation 3:

$$Q_{inf} = f_c \times (B \times L + h\,(B + L)) \tag{3}$$

where: Q_{inf} – stormwater infiltration flux into the soil, varying over time t, (m^3/s), f_c – infiltration rate, (mm/hr), B – width of the infiltration trench, (m), L – length of the infiltration trench, (m), h – water depth in the soil, (m).

To develop the surface runoff model $Q_{outS} = f(t)$, the kinematic wave equation (Akan, 1993) was used, defined as Equation 4:

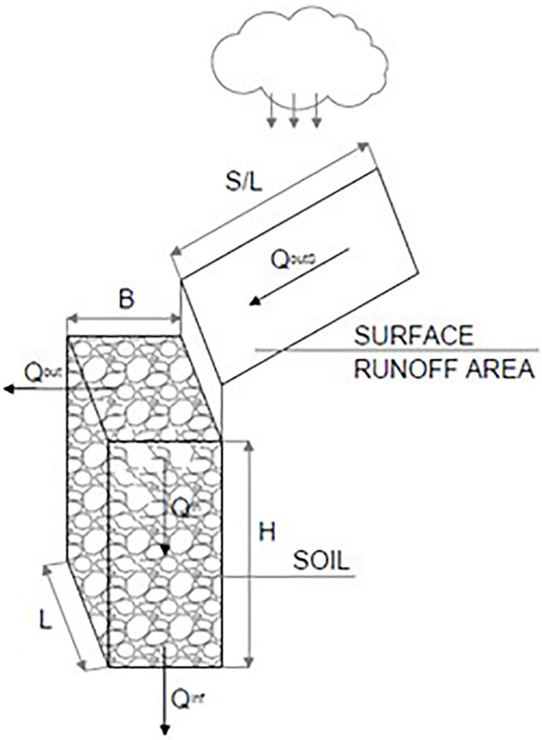

Figure 2. Schematic representation of the infiltration system

$$\frac{\partial q}{\partial x} + \frac{\partial y}{\partial t} = i - f \tag{4}$$

where: $\frac{\partial q}{\partial x}$ – flow gradient in the spatial direction, $\frac{\partial y}{\partial t}$ – change in water depth over time, i – rate of rainfall, (expressed in mm/hr), f – rate of losses from rainfall.

Taking into account the relationship $R_h = y$, where y is the thickness of the water layer (m), Equation 4 allows for modelling phenomena related to stormwater runoff over a flat surface. In a practical context, the solution of the equation allows for considering the impact of rainfall intensity and the actual infiltration rate on surface runoff processes.

According to Darcy-Weisbach's Equation 5 and 6, the friction slope S_f is calculated using the following equation:

$$S_f = \frac{f_d \cdot V^2}{8 \cdot g \cdot R_h} \tag{5}$$

for:

$$f_d = \frac{C}{Re} \tag{6}$$

where: S_f, S_0 – friction slop,(-), R_h – hydraulic radius, (m), f_d – friction factor, (-), V – average flow velocity, (m/s), C – laminar flow resistance factor, (-), Re – Reynolds number, (-), υ – kinematic viscosity of the water, (m^2/s).

The computational methodology for surface runoff is detailed in Supplementary Information – S1 Section.

At the same time, the application calculates rainwater outflow from the soil through drainage pipes, as described by Equation 7:

$$\varepsilon \cdot B \cdot L \cdot \frac{dh}{dt} = Q_{outS}(t) - Q_{out}(t) \tag{7}$$

where: ε – porosity coefficient, (-), B – width of the infiltration trench, (m), L – length of the infiltration trench, (m), dh/dt – change in water depth in the soil over time, Q_{outS} – inflow rate of stormwater to the trench, variable over time t, (m^3/s), Q_{out} – runoff rate of sewer system, variable over time t, (m^3/s).

For the saturation zone, the runoff through the drainage pipe is described by the following relationships (8) and (9):

$$Q_{out} = \frac{-\left(\frac{h + D}{L \cdot B \cdot K}\right) + \sqrt{\left(\frac{h + D}{L \cdot W \cdot K}\right)^2 + 4 \cdot N \cdot H}}{2 \cdot N} \tag{8}$$

for:

$$N = \frac{f \cdot L}{2 \cdot g \cdot A_{pipe}^2 \cdot D} + \frac{1}{2 \cdot g \cdot A_{pipe}^2} + \\ + \frac{C_L}{2 \cdot g \cdot A_{pipe}^2 \cdot \Theta_{agg}^2} \tag{9}$$

where: H – thickness of the water table in the soil, (m), h – thickness of the soil above the top of the pipe, (m), D – inner diameter of the pipe, (m), L – length of the infiltration trench, (m), K – hydraulic conductivity of soil, (m/s), B – width of the infiltration trench, (m), A_{pipe} – cross-sectional area of the pipe, (m^2), Θ_{agg} – porosity of the soil, (-), C_L – coefficient of local resistances, (-), g – gravitational acceleration, (m/s^2), λ – linear resistance coefficient, (-), calculated using the formula (10):

$$\lambda = \frac{1}{\left(-2 \cdot log\left(\frac{k}{3.71 \cdot D}\right)\right)^2} \tag{10}$$

where: k – roughness of the conduit, (m), D – inner diameter of the pipe, (m).

The runoff through the drainage pipe, assuming no saturation of the soil (11):

$$Q_{out} = \\ = \frac{-\left(\frac{L}{\left(H + \frac{D}{2}\right) \cdot K}\right) + \sqrt{\left(\frac{L}{K \cdot \left(H + \frac{D}{2}\right)}\right)^2 + 4 \cdot N \cdot H}}{2 \cdot N} \tag{11}$$

One of the alternatives for runoff from the catchment area is the triangular hydrograph, which is described in detail in S2 Section.

Rainfall data for designing an infiltration trench

The analysis aimed to identify the representative rainfall duration that maximized the retention capacity of infiltration trenches, as outlined by Akan and Houghtalen (2003). Rainfall events with durations ranging from t_d = 15 to 240 minutes were analyzed at 5-minute intervals, with rainfall depth calculated using the relationship described in Equation 1.

Input data for the calculations of the infiltration trench, catchment and runoff

The study evaluated the impact of rainfall data on the design and dimensions of infiltration trenches. Specifically, it sought to determine the optimal duration of convective rainfall events for achieving maximum retention capacity. Rainfall depths were calculated for durations ranging from 15 to 240 minutes, using 5-minute increments, based on the relationship outlined in Equation 1. The following input data were used in the application, as shown in Table 1.

Calculation assumptions (representative rainfall duration time)

The computational algorithm used in this study for the design of NBS objects includes the following forecasts: Surface runoff: calculations were performed based on empirical coefficients a_1, a_2, and a_0 (S1 Table).

Capacity of the infiltration trench: a simulation of the infiltration trench was carried out based on the input parameters, such as trench length B = 3.0 m and trench width L = 20 – 400 m. Runoff was also simulated considering the input data presented in Table 1 for runoff.

RESULTS

Rainfall duration and infiltration trench capacity

The relationship between rainfall duration and infiltration capacity is shown in Figure 3, which highlights the dynamics of the infiltration process across different locations.

The analysis covered infiltration trench dimensions in 32 selected cities across Poland, focusing on how rainfall duration influences retention capacity. The study found significant similarities in infiltration capacities across various mesoregions. The highest infiltration capacity was recorded during a 15-minute convective rainfall event in Nowy Sącz (86 m^3). As rainfall duration increased, infiltration capacity decreased, reaching as low as 2 m^3 for a 130-minute rainfall event.

In mesoregion 6, Nowy Sącz displayed the highest infiltration capacity (86 m^3), while Zakopane, also in mesoregion 6, recorded the lowest value (37 m^3). The highest infiltration capacity in Nowy Sącz corresponded with the highest stormwater flooding sensitivity index (p_s), as reported by Szeląg et al. (2022b). Conversely, Elbląg showed the lowest sensitivity index (p_s = 0.20). Furthermore, the study observed that mountainous areas like Nowy Sącz, which have a high infiltration capacity and sensitivity index, are more prone to flooding during intense rainfall events. For small urban catchments with an imperviousness

Table 1. Assumed input data used for the infiltration trench, catchment, and runoff (Akan and Houghtalen, 2003)

Name	Index	Unit	Value
Infiltration trench			
Rainfall duration	t_d	min	15–240 (step 5 min)
Porosity coefficient	ε	-	0.44
Infiltration rate	fc	m/s	0.001
Width	B	m	3
Length	L	m	20–400 (step 1 m)
Catchment			
Width of flow path	B	m	10
Length of flow path	L	m	20
Manning's roughness coefficient	n	$m^{-1/3}\cdot s$	0.0015
Hydraulic gradient	S_0	-	0.001
Runoff			
Maximum water depth in the soil	h	m	1.5
Diameter of drainage pipes	D	m	0.15
Hydraulic conductivity of soil	K	m/s	0.15
Cross-sectional area of the pipe	A_{pipe}	m^2	0.01766
Porosity of the soil	Θ_{agg}	-	0.3
Coefficient of local resistances	CL	-	1
Roughness of the conduit	k	m	0.001

coefficient (Imp) of 0.36, these factors underline the necessity of integrating flood risk management and land-use planning to mitigate flooding and support sustainable development.

In mesoregion 3, the infiltration capacities exhibited notable uniformity. During a 15-minute rainfall event, the average infiltration capacity ranged from 48.8 m^3 (5th percentile) to 77 m^3 (90th percentile). Extending the rainfall duration to 30 and 60 minutes resulted in a reduction in infiltration capacities to 46 m^3 and 26 m^3, respectively.

In comparison, mesoregion 1 showed lower infiltration trench capacities. For a 15-minute rainfall event, the average infiltration capacity

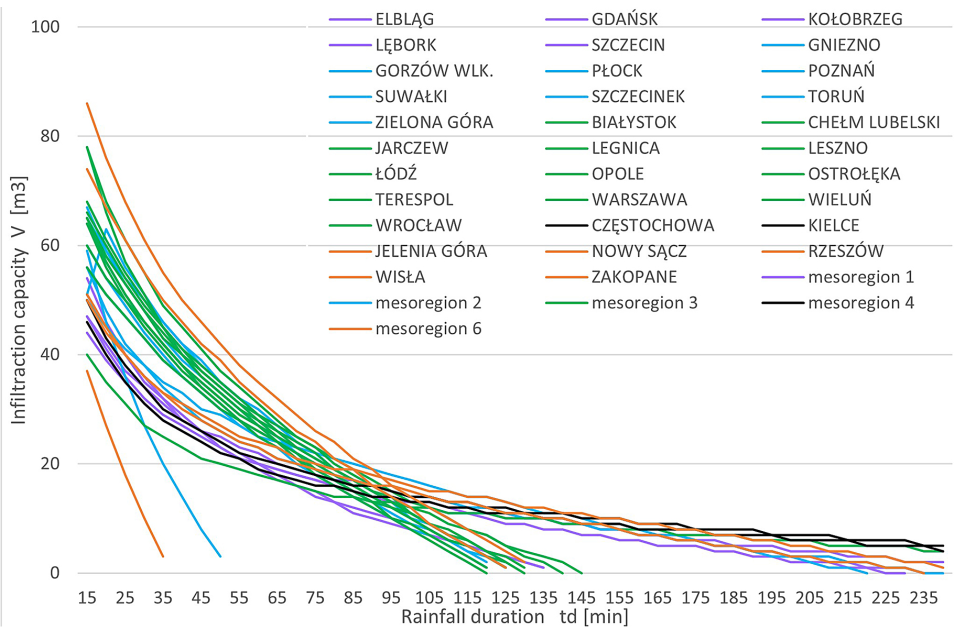

Figure 3. Effect of rainfall duration on the infiltration capacity

ranged from 44.6 m³ (5th percentile) to 52.8 m³ (90th percentile). When the rainfall duration increased to 30 and 60 minutes, the infiltration capacities declined to 34 m³ and 20 m³, respectively.

The relationship between rainfall duration and infiltration trench capacity underscores the need for improved stormwater monitoring and adaptive management, particularly in regions with lower retention capacity. The findings from Polish studies indicate that prolonged rainfall durations significantly diminish soil infiltration capacity. For instance, in mesoregion 1, the infiltration capacity for a 60-minute rainfall event is reduced to 20 m³ – less than half of the capacity observed for a shorter, 15-minute event. These results highlight the challenges cities may face in managing stormwater during extended rainfall events, necessitating tailored strategies to optimize urban drainage systems and prevent flooding.

The variations in infiltration trench capacities across cities and mesoregions are presented in Figure 4, demonstrating the spatial diversity in stormwater retention performance.

The analysis of infiltration trench capacity (*V*) in selected Polish cities revealed significant differences across various mesoregions. These findings are crucial for evaluating retention potential and optimizing water infrastructure planning at the national scale. Mesoregion 1 (Baltic Lakeland): Cities such as Szczecin (54 m³), Gdańsk (51 m³), and Elbląg (44 m³) exhibited lower infiltration capacities compared to other regions. Mesoregion 2: This region showed higher values, with cities like Gniezno (51 m³), Gorzów Wielkopolski (56 m³), and Płock (59 m³). Zielona Góra (67 m³) and Suwałki (65 m³) recorded the highest capacities within this region. Mesoregion 3 (Central and Eastern Poland): Higher capacities were observed, with Jarczew and Chełm Lubelski reaching 78 m³. Other cities, such as Legnica (68 m³) and Opole (66 m³), also demonstrated favorable retention capabilities, while Wieluń recorded the lowest value at 40 m³. Central cities like Częstochowa (50 m³) and Kielce (46 m³) had relatively low capacities. Mesoregion 6 (Mountainous Terrain): The highest values in Poland were recorded here, with Nowy Sącz achieving 86 m³ and Rzeszów 74 m³. However, Zakopane had the lowest capacity in the country at 37 m³, highlighting the region's variability due to its topographic conditions.

Rainfall intensity and its impact on infiltration capacity of soil in small urban catchment in Poland

Rainfall intensity analysis identified five intensity levels, highlighting areas with both heavy and moderate rainfall. The results are presented in Figure 5.

The highest recorded rainfall intensities, exceeding 50 mm/min, were observed in four cities: Chełm Lubelski (53.8 mm/min), Jarczew (53.7 mm/min), Rzeszów (51.3 mm/min), and Nowy Sącz (59.3 mm/min, the highest value, located in mesoregion 6). Rainfall intensities in the range

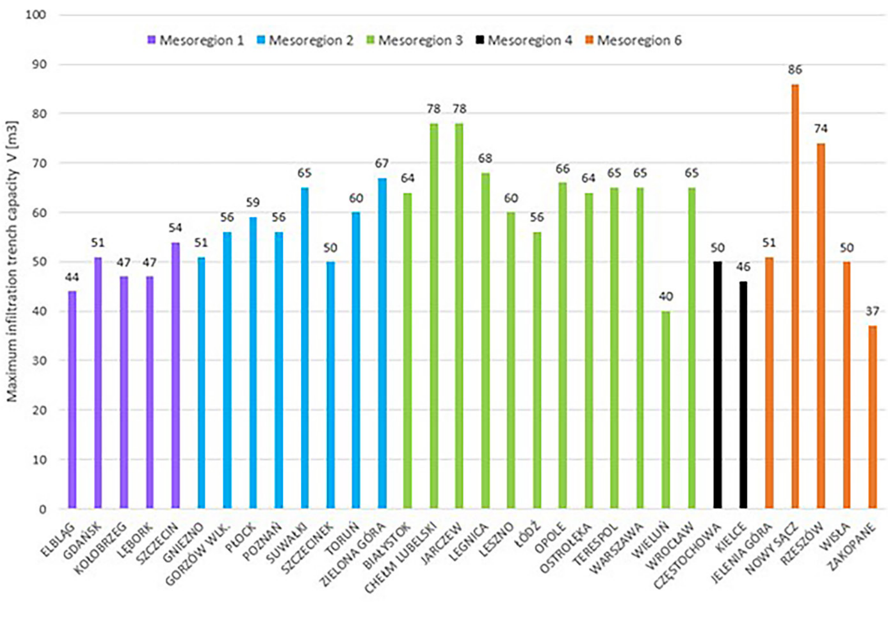

Figure 4. Maximum infiltration trench capacity V (m³) for individual cities

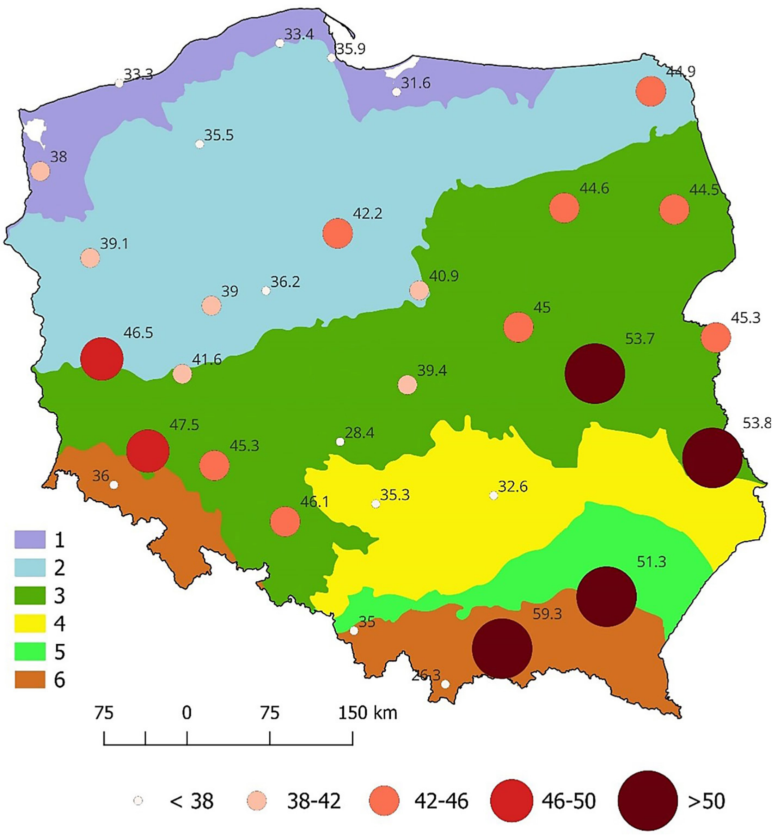

Figure 5. Representative rainfall intensity

of 46–50 mm/min were recorded in three cities: Legnica, Opole, and Zielona Góra. Seven cities: Białystok, Ostrołęka, Suwałki, Terespol, Toruń, Warsaw, and Wrocław; fell within the 42–46 mm/min range. Five cities: Gorzów Wielkopolski, Leszno, Łódź, Płock, and Poznań; reported values in the 38 – 42 mm/min range. The largest group comprised 13 cities with rainfall intensities below 38 mm/min, including Częstochowa, Elbląg, Gdańsk, Gniezno, Jelenia Góra, Kielce, Kołobrzeg, Lębork, Szczecin, Szczecinek, Wieluń, Wisła, and Zakopane, where the lowest value of 26.3 mm/min was recorded. A comparative analysis with Szeląg et al. (2022b) reveals a clear association between cities experiencing the highest rainfall intensities and areas identified as having a high vulnerability index for runoff in small catchments. Cities such as Nowy Sącz, Chełm Lubelski, Jarczew, and Rzeszów, which recorded the highest rainfall intensities, also demonstrated the highest sensitivity index values (p_s > 0.5) in Szeląg's study. This indicates that regions prone to intense, short-duration rainfall events are particularly susceptible to frequent and extensive flooding. These findings underscore the importance of incorporating local hydrological variability into flood risk management and forecasting frameworks. The impact of localized rainfall conditions is further confirmed by De Martino et al. (2010) in their study of the Campania region (Italy), which illustrates that regression models based on local rainfall data can effectively predict sewage system loads and water quality during heavy rainfall events. Similarly, De Paola et al. (2012) examined the relationships between rainfall characteristics, the geographical locations of the studied stations, and the unit capacities of the tanks analyzed in the same country. In Poland, cities such as Nowy Sącz and Rzeszów, where stormwater drainage systems are especially vulnerable to overloading, could benefit from adopting similar approaches to enhance stormwater management efficiency. Furthermore, an analysis was conducted on the performance of an infiltration trench with a maximum length of 3.0 m. The results are presented in Figure 6.

Analyzing the infiltration trench capacity for a maximum length of 3.0 meters, the results align with the spatial distribution presented in Figure 6. The highest infiltration capacities, exceeding 70 m^3, were observed in Nowy Sącz (86 m^3), Chełm Lubelski (78 m^3), Jarczew (78 m^3), and Rzeszów

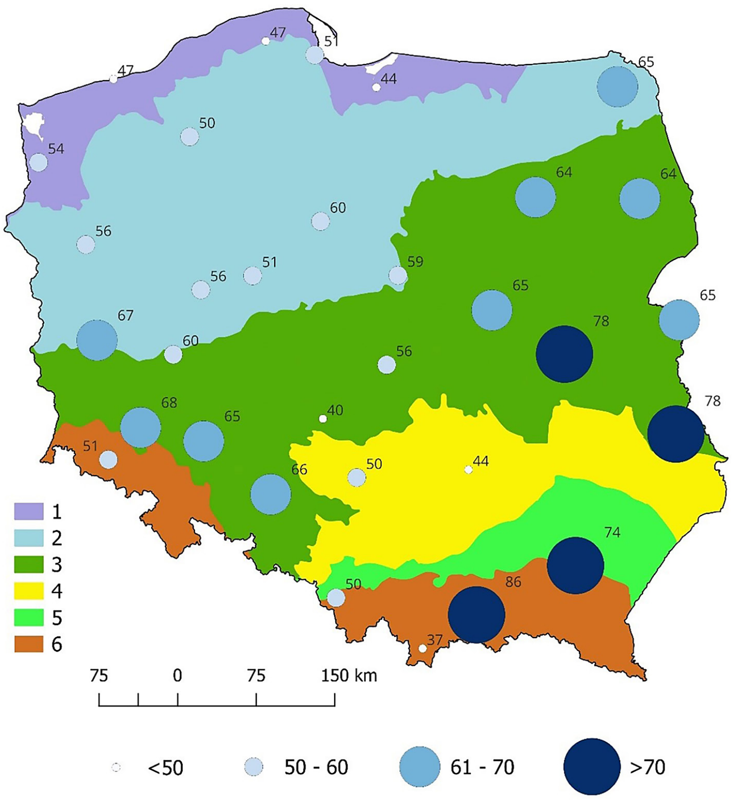

Figure 6. Infiltration trench capacity

(74 m³). These four cities, situated in mesoregions 6 and 3, exhibit the greatest retention capacities.

Infiltration capacities within the range of 61–70 m³ were recorded in six cities: Legnica, Zielona Góra, Opole, Suwałki, Terespol, and Warsaw, as well as Białystok and Ostrołęka. These cities are primarily located in central Poland, within mesoregions 3 and 2.

The largest group, comprising 13 cities, displayed infiltration capacities between 50 and 60 m³. These cities include Leszno, Toruń, Płock, Gorzów Wielkopolski, Łódź, Poznań, Szczecin, Gdańsk, Gniezno, Jelenia Góra, Częstochowa, Szczecin, and Wisła. Conversely, cities with infiltration capacities below 50 m³ included Kołobrzeg, Lębork, Kielce, Elbląg, Wieluń, and Zakopane, with Zakopane recording the lowest value of 37 m³.

In terms of mesoregional characteristics, distinct variations in rainfall and infiltration capacities are evident. Mesoregions 1 and 4 are associated with the lowest rainfall intensities (below 38 mm/min) and moderate soil capacities (44–54 m³ and 46–50 m³, respectively), promoting hydrological stability. Mesoregion 2 experiences moderately higher rainfall (35.5–46.5 mm/min) and larger soil capacities (50–67 m³), supporting improved water retention. Mesoregion 3 exhibits high variability in rainfall (28.4 – 53.8 mm/min) and soil capacity (40–78 m³). Mesoregion 6, which experiences the highest rainfall intensities (35–59.3 mm/min), also demonstrates the greatest soil capacity (50–86 m³).

These findings corroborate the results of Szeląg et al. (2022b), which emphasized that physical and geographical conditions, along with localized rainfall patterns, significantly influence the maximum permissible impermeability limit. This limit defines the threshold rainfall intensity, exceeding which triggers the occurrence of wastewater discharge in the catchment, depending on the area's impermeability. Exceeding this threshold often results in stormwater system overflows within small urban catchments. A comparison of infiltration trench capacities across Poland reveals notable differences and significant correlations between mesoregions. The greatest variability is observed in Mesoregion 1 (Baltic coast), characterized by low retention capacity but an imperviousness value (Imp_{gr}: 0.51 – 0.56), as described by Szeląg at al. (2022b). Limited water retention in this region, coupled with intense surface runoff driven by urbanization and impermeable soils, exacerbates the challenges of water absorption. Consequently, the design and implementation of efficient stormwater management systems, such as retention tanks, infiltration trenches, and irrigation systems (NSN), are crucial in this area.

Implications of the use of green infrastructure in urban catchments

An integrated approach to stormwater management that combines GI with traditional stormwater systems and retention tanks represents a modern and effective strategy for mitigating surface runoff and improving the operational efficiency of stormwater systems. Jing et al. (2024) and Szelag et al. (2024) have substantiated that the synergistic application of both natural and engineered systems can substantially diminish flood risk and contribute to the enhancement of surface water quality.

Within the context of urban catchments, GI assumes a pivotal role in stormwater management, climate change adaptation, and water quality improvement. Research by Almaaitah (2024) demonstrated that green roofs can retain up to 63% of rainfall, while retention farms can achieve retention rates of 85–88%, which not only attenuates surface runoff but also mitigates water levels in retention tanks. Moreover, studies by Cavadini et al. (2024) in Switzerland have confirmed that bioretention infiltration zones can reduce the volume of stormwater overflows by as much as 52% in scenarios involving a 46% increase in rainfall, providing evidence that GI can effectively address the challenges associated with intensified rainfall events.

Hepcan and Canguzel (2024) evaluated GI in the context of hydrometeorological risk reduction in Izmir, highlighting that optimizing GI systems enhances water retention and fortifies urban resilience. Matías Rodríguez et al. (2024) demonstrated that green roofs and permeable pavements can augment the resilience of combined stormwater systems by 9–22%, effectively reducing stormwater overflows. Furthermore, the appropriate design of hydraulic structures has been shown to reduce peak stormwater runoff and curb soil erosion. Empirical evidence confirms that GI enhances the hydrological balance, supports biodiversity, mitigates the urban heat island effect, and reduces the burden on sewer infrastructure.

GI also exerts a positive influence on the quality of wastewater discharged into receiving water bodies. Cavadini et al. (2024) confirmed that bioretention systems can substantially decrease the concentration of pollutants, thereby improving the quality of urban waters and supporting local water resources.

Additionally, further research underscores the political and urban planning dimensions of GI. Sowby et al. (2024) emphasized the imperative to implement climate-resilient standards in water infrastructure, drawing on case studies from Copenhagen and Melbourne. Zhu et al. (2024) demonstrated that effective GI policy necessitates the integration of assessment metrics and environmental regulatory frameworks.

CONCLUSIONS

The proposed application has proven effective in addressing critical engineering and scientific challenges on a national scale, particularly in the field of stormwater management within small urban catchments. Its versatility allows for the evaluation of equations under varied assumptions and conditions, making it applicable to the design of retention tanks, the dimensioning of infiltration systems, and the modernization of stormwater infrastructure.

The analysis of data from 32 cities reveals significant disparities in rainfall intensity and the retention capacities of infiltration systems. Convective rainfall events are shown to maximize system capacity, while prolonged rainfall gradually diminishes their effectiveness. Cities such as Nowy Sącz, Chełm Lubelski, Jarczew, and Rzeszów exhibit high retention capacities, whereas cities like Elbląg, Wieluń, and Zakopane record the lowest values.

These findings emphasize the necessity of adopting localized approaches to stormwater system design, tailored to the unique geological and climatological characteristics of different mesoregions. Such strategies are essential for improving flood protection and ensuring sustainable water resource management, especially in light of increasing climate variability.

The developed tool and the insights gained from this study represent a significant advancement in enhancing urban resilience to extreme weather events. This work contributes to the sustainable development of urban ecosystems and the promotion of hydrological safety, both in Poland and globally.

Acknowledgements

This research was funded by internal projects at Lublin University of Technology, Poland numbers FD-20/IS-6/024.

REFERENCES

1. Akan, A.O. (1993). *Urban Stormwater hydrology* – A Guide to Engineering Calculations, Technomic, Lancaster, PA.
2. Akan, A.O., & Houghtalen, R.J. (2003). *Urban Hydrology, Hydraulics, and Stormwater Quality: Engineering Applications and Computer Modelling;* John Wiley & Sons, Inc.: Hoboken, NJ, USA.
3. Almaaitah, T. (2024). Multifunctional blue-green infrastructure and low impact development for climate change adaptation. https://doi.org/10.32920/26883574.v1
4. Bhaskar, A.S., Hogan, D.M., & Archfield, S.A. (2016). Urban base flow with low impact development. *Hydrological Processes*, *30*(18), 3156–3171. https://doi.org/10.1002/hyp.10808
5. Beven, K.J. (2012). *Rainfall-runoff modelling: the primer*. John Wiley & Sons
6. Błażejewski, R., Nieć, J., Murat-Błażejewska, S., & Zawadzki, P. (2018). Comparison of infiltration models with regard to design of rectangular infiltration trenches. *Hydrological Sciences Journal, 63*(11), 1707–1716. https://doi.org/10.1080/02626667.2018.1523616
7. Boogaard, F., & Kondratenko, J. (2024). Low impact development devices DNA of cities for long term stormwater management strategies. *Discover Water*, *4*(34). https://doi.org/10.1007/s43832-024-00090-0
8. Cavadini, G. B., Rodríguez, M., Nguyen, T., & Cook, L. M. (2024). Can blue-green infrastructure counteract the effects of climate change on combined sewer overflows? study of a swiss catchment. Environmental Research Letters. https://doi.org/10.1088/1748-9326/ad6462
9. Chan, F.K.S., Griffiths, J.A., Higgitt, D., Xu, S., Zhu, F., Tang, Y.T., et al. (2018). "Sponge City" in China – A breakthrough of planning and flood risk management in the urban context. *Land Use Policy*, *76*, 772–778. https://doi.org/10.1016/j.landusepol.2018.03.005
10. Chen, V., Bonilla Brenes, J. R., Chapa, F., & Hack, J. (2021). Development and modelling of realistic retrofitted Nature-based Solution scenarios to reduce flood occurrence at the catchment scale. *Ambio*, *50*, 1462–1476. https://doi.org/10.1007/s13280-020-01493-8
11. Chow, V.T., Maidment, D.R., & Mays, L.W. (1988). Applied Hydrology; McGrawl-Hill Book Company: New York, NY, USA.
12. City of Melbourne (2012) Melbourne (Vic.). Council; Urban Forest Strategy 2012.
13. Czerpak, J., & Widomski, M.K. (2024). Numerical assessment of green infrastructure influence on hydrologic effectiveness in a suburban residential development. *Journal of Ecological Engineering*, *25*(7), 187–200. https://doi.org/10.12911/22998993/188364
14. Davis, A.P., Traver, R.G., Hunt, W.F., Lee, R., Brown, R.A., & Olszewski, J.M. (2012). Hydrologic Performance of Bioretention Storm-Water Control Measures. *Journal of Hydrologic Engineering*, *17*(5), 604–614. https://doi.org/10.1061/(ASCE)HE.1943-5584.0000467
15. De Martino, G., De Paola, F., Fontana, N., Marini, G., & Ranucci, A. (2010). Preliminary design of combined sewer overflows and stormwater tanks in Southern Italy. *Irrigation and Drainage*, *60*(4), 544–555. https://doi.org/10.1016/j.proenv.2013.06.013
16. Denault, C., Millar, R.G., & Lence, B.J. (2006). Assessment of Possible Impacts of Climate Change in an Urban Catchment. *Journal of the American Water Resources Association*, *42*(3), 685–697. https://doi.org/10.1111/j.1752-1688.2006.tb04485.x
17. De Paola, F., Ranucci, A. (2012). Analysis of spatial variability for stormwater capture tank assessment. *Irrigation and Drainage*, *61*, 682–690. https://doi.org/10.1002/ird.1675
18. DWA-A 118E. (2006) Hydraulic Dimensioning and Verification of Drain. and Sewer Systems, DWA German Association for Water, Wastewater and Waste, Hennef, Germany
19. European Commission. (2015). Towards an EU Research and Innovation policy agenda for nature-based solutions and renaturing cities. Final Report of the Horizon 2020 Expert Group on Nature-Based Solutions and Re-naturing Cities. Brussels: European Commission. https://doi.org/10.2777/479582
20. Farina, A., Di Nardo, A., Gargano, R., van der Werf, J.A., & Greco, R. (2023). A simplified approach for the hydrological simulation of urban drainage systems with SWMM. *Journal of Hydrology*, *623*, 129757. https://doi.org/10.1016/j.jhydrol.2023.129757
21. Gill, S., Handley, J., Ennos, A., & Pauleit, S. (2007). Adapting cities for climate change: The role of the green infrastructure. *Built Environment*, *33*(1), 115–133. https://doi.org/10.2148/benv.33.1.115
22. Hansen, L., Borup, M., Møller, A., & Mikkelsen, P. (2014). Flow forecasting using deterministic updating of water levels in distributed hydrodynamic

urban drainage models. *Water*, *6*(8), 2195–2211. https://doi.org/10.3390/w6082195

23. Hatt, B., Fletcher, T., Walsh, C.J. & Taylor, S.L. (2004). The influence of urban density and drainage infrastructure on the concentrations and loads of pollutants in small streams. *Environmental Management*, *34*, 112–124. https://doi.org/10.1007/s00267-004-0221-8
24. Hepcan, Ç., & Canguzel, A. (2024). The impact of blue-green infrastructure on climate resilience for hydrometerological hazards: The case of Bayraklı, İzmir. *Deleted Journal*. https://doi.org/10.58816/duzceod.1413255
25. Imran, H.M., Kala, J., Ng, A.W.M., & Muthukumaran, S. (2018). Effectiveness of green and cool roofs in mitigating urban heat island effects during a heatwave event in the city of Melbourne in southeast Australia. *Journal of Cleaner Production*, *197*(1), 393–405. https://doi.org/10.1016/j.jclepro.2018.06.179
26. Jiang, Y., Zevenbergen, C., & Ma, Y. (2018). Urban pluvial flooding and stormwater management: A contemporary review of China’s challenges and “sponge cities” strategy. *Environmental Science & Policy*, *80*, 132–143. https://doi.org/10.1016/j.envsci.2017.11.016
27. Jing, J., Hou, J., Pan, Z. et al. (2024). Simulation and Evaluation of Collapsible Risk of Low Impact Development Rainwater System in Collapsible Loess Area. *Water Resour Manage 38*, 5485–5505. https://doi.org/10.1007/s11269-024-03896-8
28. Kabisch, N., Korn, H., Stadler, J., & Bonn, A. (2017). *Nature-Based Solutions to Climate Change Adaptation in Urban Areas—Linkages Between Science, Policy and Practice*. In: Kabisch, N., Korn, H., Stadler, J., Bonn, A. (eds) Nature-Based Solutions to Climate Change Adaptation in Urban Areas. Theory and Practice of Urban Sustainability Transitions. Springer, Cham. https://doi.org/10.1007/978-3-319-56091-5_1
29. Kaczmarek, Z., & Kaczmarek, A. (2019). Spatial distribution of precipitation in Poland. *Geographical Journal*, *31*(2), 125–139.
30. Kupczyk E. & Suligowski R. (1997). *Statistical description of the rainfall structure as the input to hydrological models*. In Prediction of the design storms and floods; Soczyńska U. (Ed.), University of Warsaw Publisher: Warsaw, 191–212
31. Kupczyk E. & Suligowski R. (2000). Temporal and spatial patterns of high intensity rainfalls in Poland. *Miscellanea Geographica*, *9*, 77–84. https://doi.org/10.2478/mgrsd-2000-090110
32. Łazuka, E., Futa, A., Jastrzębska, M., Łagód, G., Szeląg, B., & Fatone, F. (2022). The applications of graph algorithms to modeling of integrated urban water management system. *Advances in Science and Technology Research Journal*, *16*(5), 277–89. https://doi.org/10.12913/22998624/155037
33. Łupikasza E. (2016). *The climatology of air-mass and frontal extreme precipitation*. Study of meteorological data in Europe. Springer International Publishing AG Switzerland.
34. Maimone, M., O’Rourke, D.E., Knighton, J.O., & Thomas, C.P. (2011). Potential Impacts of Extensive Stormwater Infiltration in Philadelphia. *Environmental Engineer and Scientist*: *Applied Research and Practice*, *14*, 29–39.
35. Mailhot, A., Lachance-Cloutier, S., Talbot, G., & Favre, A.C. (2013). Regional estimates of intense rainfall based on the Peak-Over-Threshold (POT) approach. *Journal of Hydrology*, *476*, 188–199. https://doi.org/10.1016/j.jhydrol.2012.10.036
36. Marchioni, M., & Becciu, G. (2018). Infiltration-exfiltration system for stormwater runoff volume and peak attenuation. *International Journal of Safety and Security Engineering*, *8*(4). https://doi.org/10.2495/SAFE-V8-N4-473-483
37. Miller, J.D., Kim, H., Kjeldsen, T.R., Packman, J., Grebby, S., & Dearden, R. (2014). Assessing the impact of urbanization on storm runoff in a peri-urban catchment using historical change in impervious cover. *Journal of Hydrology*, *515*, 59–70. https://doi.org/10.1016/j.jhydrol.2014.04.011
38. Musz-Pomorska, A., & Widomski, M.K. (2022). Analysis of the impact of the degree of catchment sealing on the operation of drainage system. *Applied Water Science*, *12*(11), 1–9. https://doi.org/10.1007/s13201-022-01774-5
39. Niedźwiedź, T., Twardosz, R., Walanus, A. (2009). Long-term variability of precipitation series in east central Europe in relation to circulation patterns. *Theoretical and Applied Climatology*, *98*, 337–350. https://doi.org/10.1007/s00704-009-0122-0
40. Piazza, P.; & Ursino, N. (2022). Modelling infiltration systems’ performance for efficient, sustainable or circular urban water drainage. *Water*, *14*, 2620. https://doi.org/10.3390/w14172620
41. Procaccini, G., & Monticelli, C. (2021). A green roof case study in the urban context of milan: integrating the residential and cultivation functions for sustainable development. *Water*, *13*(2), 137. https://doi.org/10.3390/w13020137
42. Raymond, C.M., Frantzeskaki, N., Kabisch, N., Berry, P., Breil, M., Nita, M. R., & et al. (2017). A framework for assessing and implementing the co-benefits of nature-based solutions in urban areas. *Environmental Science & Policy*, *77*, 15–24. https://doi.org/10.1016/j.envsci.2017.07.008
43. Rodríguez, M. M., Fu, G., Butler, D., Yuan, Z., & Cook, L. (2024). The effect of green infrastructure on resilience performance in combined sewer

systems under climate change. *Journal of Environmental Management, 353*, 120229. https://doi.org/10.1016/j.jenvman.2024.120229

44. Salerno, F., Valsecchi, L., Minoia, R., Copetti, D., Tartari, G., Guyennon, N., Colombo, N., Pirola, N., Barozzi, B., Bellazzi, A., & Marziali, L. (2021). Factors Controlling the Hydraulic Efficiency of Green Roofs in the Metropolitan Area of Milan (Italy). *Sustainability*, *13*(24), 13638. https://doi.org/10.3390/su132413638
45. Sanesi, G., Colangelo, G., Lafortezza, R., Calvo, E., & Davies, C. (2016). Urban green infrastructure and urban forests: a case study of the Metropolitan Area of Milan. *Landscape Research*, *42*(2), 164–175. https://doi.org/10.1080/01426397.2016.1173658
46. Shariat, R., Roozbahani, A., & Ebrahimian, A. (2019). Risk analysis of urban stormwater infrastructure systems using fuzzy spatial multi-criteria decision making. *Science of The Total Environment*, *647*, 1468–1477. https://doi.org/10.1016/j.scitotenv.2018.08.074
47. Singh, V. P. (1996). *Kinematic Wave Modeling in Water Resources*: Surface Water Hydrology. John Wiley & Sons
48. Song, C. (2022). Application of nature-based measures in China's sponge city initiative: Current trends and perspectives. *Nature-Based Solutions*, *2*, 100010. https://doi.org/10.1016/j.nbsj.2022.100010
49. Sowby, R. B., Jones, D., & George, G. (2024). Policy options to support climate-conscious urban water planning. *Earth, 5*(4), 896–903. https://doi.org/10.3390/earth5040045
50. Szeląg, B., Łagód, G., Musz-Pomorska, A., Widomski, M.K., Stránský, D., Sokáč, M., Pokrývková, J., & Babko, R. (2022a). Development of rainfall-runoff models for sustainable stormwater management in urbanized catchments. *Water*, *14*(13), 1997. https://doi.org/10.3390/w14131997
51. Szeląg, B., Suligowski, R., Łagód, G., Łazuka, E., Wlaź, P., Strańsky,´ D., & et al. (2022b). Flood occurrence analysis in small urban catchments in the context of regional variability. *PLOS ONE*, *17*(11), e0276312. https://doi.org/10.1371/journal.pone.0276312
52. Szeląg, B., Suligowski, R., De Paola, F., Siwicki, P., Majerek, D., & Łagoód, G. (2022c). Influence of urban catchment characteristics and rainfall origins on the phenomenon of stormwater flooding: Case study. *Environmental Modelling & Software, 150*, 105335. https://doi.org/10.1016/j.envsoft.2022.105335
53. Szeląg, B., Fatone, F., Kiczko, A., Majerek, D., Białek, A., Łagód, G., Piotrowicz, A., Dąbek, L. (2024). Extended evaluation of the impact of rainfall, sewer network and land use retention on drainage system performance in a multi-criteria approach – modeling, sensitivity analysis. *Advances in Science and Technology Research Journal. 18*(6), 291–303. https://doi.org/10.12913/22998624/192023
54. Taguchi, V.J., Weiss, P.T., Gulliver, J.S., Klein, M.R., Hozalski, R.M., Baker, L.A & et al. (2020). It is not easy being green: recognizing unintended consequences of green stormwater infrastructure. *Water*, *12*(2), 522. https://doi.org/10.3390/w12020522
55. Ursino, N. (2015). Risk analysis of sustainable urban drainage and irrigation. *Advances in Water Resources*, *83*, 277–284. https://doi.org/10.1016/j.advwatres.2015.06.011
56. US EPA. (2015). Storm Water Management Model (SWMM)
57. Wang, S., & Wang, H. (2018). Extending the Rational Method for assessing and developing sustainable urban drainage systems. *Water Research*, *144*, 112–125. https://doi.org/10.1016/j.watres.2018.07.022
58. Wu, T., Song, H., Wang, J., & Friedler, E. (2020). Framework, Procedure, and Tools for Comprehensive Evaluation of Sustainable Stormwater Management: A Review. *Water*, *12*(5), 1231. https://doi.org/10.3390/w12051231
59. Xing, Y., Ni, G., Yang, L., Yang, Y., Xing, P., & Sun, T. (2019). Modeling the impacts of urbanization and open water surface on heavy convective rainfall: A case study over the emerging Xiong'an City, China. *ournal of Geophysical Research: Atmospheres, 124*, 9078–9098. https://doi.org/10.1029/2019JD030359
60. Zhang, C., He, M., & Zhang, Y. (2019). Urban sustainable development based on the framework of Sponge City: 71 case studies in China. *Sustainability*, *11*(6), 1544. https://doi.org/10.3390/su11061544
61. Zhu, X., Zhang, Y., Zhu, H., & Zhao, W. (2024). Systematic review and research frontier analysis of urban green infrastructure policy tools. *Fengjing Yuanlin, 31*(11), 86–93. https://doi.org/10.3724/j.fjyl.202402020082